International Journal of Multiphase Flow 98 (2018) 67–78

Contents lists available at ScienceDirect

International Journal of Multiphase Flow

journal homepage: www.elsevier.com/locate/ijmulflow

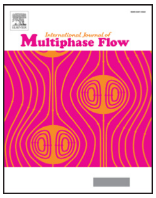

Cavitation behind a circular micro pillar

Arash Nayebzadeh*, Yingying Wang, Hanieh Tabkhi, Jeong-Heon Shin, Yoav Peles

University of Central Florida, Department of Mechanical and Aerospace Engineering, Orlando 32816 FL, United States

ARTICLE INFO

Article history:
Received 4 November 2016
Revised 9 June 2017
Accepted 26 August 2017
Available online 30 August 2017

Keywords:
Micro pillar
Hydrodynamic cavitation
Cavitation inception number
Spectral analysis

ABSTRACT

An experimental study of hydrodynamic cavitation was conducted in a rectangular microchannel with a pillar. Distilled water was used as working fluid in an open fluid loop, and cavitation was obtained by applying a range of pressure differences between inlet and outlet tanks. High speed camera captured the flow patterns from inception to fully developed cavitating flow. A minimum delay of 10 min in the formation of cavitation was recorded in all experiments, which is due to the stochastic nature of phenomenon. Cavitation inception conditions were obtained in terms of the cavitation numbers, and a flow map was developed for subsequent cavitation flow. By analyzing time series of gray scale intensity of pixels inside the cavity, dominant frequencies were identified. Transient single phase numerical simulations were performed to gain a better understanding of the flow field in the microchannel, verify pressure measurements, and to relate the separation angle to the attached cavitation angle around the pillar. Emphasis was placed on characterizing the wake region downstream the pillar as it is closely related to the occurrence of the cavitation phenomena.

1. Introduction

Hydrodynamic cavitation is often being recognized as an unfavorable phenomenon that can take place in any fluid-handling device causing a range of adverse effects, such as reduced efficiency, decreased power output, vibration, noise, surge stall, and erosion in hydraulics machineries (Arndt, 2002, 1981). At the conventional scales numerous studies have been devoted to identify, characterize, and predict cavitation in an effort to prevent its undesirable effects (Blake and Gibson, 1987; Brennen, 1995; Joseph, 1998). Studies demonstrated that cavitation can also occur at the micro scale causing damage to silicon surfaces and limiting the performance and operability of micro machines (Mishra and Peles, 2005a, b).

While cavitation is detrimental in many engineering systems, it can be beneficial in others. In electronic cooling applications, cavitation can enhance heat transfer by promoting two-phase flow and leveraging its associated high heat transfer coefficient (Schneider et al., 2007, 2006). Cavitation produced behind a micro-orifice in a microchannel can be used to eliminate leukemia cells (Koşar et al., 2011), erode kidney stones (Perk et al., 2012), and destroy prostate cells (Itah et al., 2013). Also, cell membrane disruption (Prentice et al., 2005), intensification of biological wastewater treatment (Chakinala et al., 2008a, b; Gogate and Kabadi, 2009; Gogate and Pandit, 2005; Sawant et al., 2008; Zupanc et al., 2013), food processing (Gogate, 2010), and synthesis of biodiesel (Ji et al., 2006) are some key efforts aimed at utilizing cavitation to enhance chemical mixing within biotechnology/biochemical contexts. A quick survey in the literature reveals that unlike flow boiling, there are limited studies toward cavitation at the micro scale, whereas abundant applications demand a great deal of fundamental knowledge as to how to characterize its occurrence, control it, and use its potential benefits.

Although the validity of classical fluid mechanics laws for liquids has been proven at the micro scale, appreciable deviations of cavitation in micro domains from the phenomenon in its large scale counterparts indicate the existence of strong scale effects (Amromin, 2002; Dular et al., 2012; Hsiao et al., 2003; Keller, 2001; Kuhn et al., 1995; Parkin, 1952). Such effects are the result of change in the domain shape, Reynolds number, nuclei size and distribution, reduced residence time for bubble growth, type of material used, etc. (Krishnamurthy and Peles, 2008). Furthermore, surface tension force, which dominates bubble growth (Sharp et al., 2002), is widely affected by surface and free stream nuclei at diminishing scales. A significant delay in the inception of cavitation in micro domains reported by recent studies (Medrano et al., 2011; Mishra and Peles, 2005a) is one of those scale effects. Two factors contribute to this phenomenon: (1) dominance of surface tension effect over vapor pressure in the occurrence of cavitation inception and (2) reduced residence time for bubble growth (Peles, 2008). It is also worth mentioning that viscous effects are known to be very noticeable in conventional cavitation, but because the Reynolds number in high-speed *MEMS* devices is typically low, another scal-

---

* Corresponding author.
E-mail address: arash.nayebzadeh@knights.ucf.edu (A. Nayebzadeh).

http://dx.doi.org/10.1016/j.ijmultiphaseflow.2017.08.012
0301-9322/

ing disparity arises in extending cavitation data from conventional scale to microscale.

Available literature on cavitation in micro domain is limited to micro-hydrofoils, micro-orifices, micro-venturis, and micro-diaphragms. The attempt to explore cavitation in non-conventional domains, albeit in one millimeter scales, was initiated during the micro jet engine project at MIT by Pennathur (2001). They witnessed the occurrence of cavitation in silicon micro-fabricated turbo pump around 900 µm long chord hydrofoils with working fluids like water and ethanol. They then developed design criteria for microscale turbo pumps and evaluated cavitation influence on micro pump performance. Cavitating flow in micro-orifice and in micro-venturis entrenched in rectangular silicon microchannel was studied in details by Mishra and Peles (2006, 2005a, b). They detected various cavitating flow regimes and reported several similarities and deviations between the micro and the macro scales. In particular, they observed low incipient cavitation numbers suggesting a strong scale effect. Medrano et al. (2012, 2011) conducted experiments on cavitation behind micro-venturis and micro-diaphragms with deionized water and nanofluids. They reported a delay in the onset of cavitation in all of their devices and related it to the metastability of the liquid and lack of wall roughness (i.e., surface nuclei). High-pressure microfluidic systems in the form of T-channel and orifice-channel have been studied by a photo-optical cavitation measurement technique and micro particle image velocimetry *(μPIV)* under pressure drops up to 500 bar and different regimes of hydrodynamic cavitation were characterized (Gothsch et al., 2015). Another effort in the context of characterizing cavitation patterns downstream a cylindrical coaxial orifice has been conducted through high speed imaging and acoustical measurements (Schlender et al., 2015). More recently, Cioncolini et al. (2016) focused on chocked cavitation with circular micro-orifice in different geometries and compared their findings with the previous studies in order to find a reliable trend for this type of cavitation. Signal processing techniques, such as fast Fourier transform *(FFT)* by De Giorgi et al. (2013) and wavelet decomposition by De Giorgi et al. (2015a, b), to the pressure and optical signals have been recently carried out in order to detect cavitation regimes in a millimeter-scale cylindrical orifice.

As discussed above, available literature provides insight about the nature of cavitation. However, other important geometries, such as micro-cylinders, which have not yet been explored, can produce cavitation with unique features. In recent years, micro pin fins (pillars) embedded in microchannels have gained considerable attention as a promising passive tool to foster mixing, reduce thermal boundary layer thickness, and enhance heat transfer coefficient (Kosar and Peles, 2007a, b, 2006; Koşar and Peles, 2007; Koşar et al., 2005; Krishnamurthy and Peles, 2010, 2008; Peles et al., 2005; Wang et al., 2013). At certain flow circumstances, the pressure behind a pin fin may reach the vapor pressure of a liquid, giving rise to the emergence of hydrodynamic cavitation. Such cavitating flow could be a potential source of damage and pose limitation to the functionality of the device if supercavitation or choked cavitating flow occurs. Alternatively, cavitation can be exploited as a means for heat transfer enhancement if thoroughly predicted and controlled. For electronic cooling applications, microchannel-confined pin fins with short aspect ratios and associated flow pattern behind the fin are of great interest. While flow morphology around conventional free-end bluff bodies and the effect of confinement have always been considered to be classic fluid mechanics problems, which were extensively studied by Williamson (1996) and Zdravkovich (1997), a knowledge gap still exists pertinent to the manner in which small geometries, such as micro pin fins, alter flow behavior inside a microchannel. In the case of a short cylinder confined between a top wall and a bottom wall inside a microchannel, the dynamic of the wake flow is affected mainly by the interaction between the wall shear layer and the pin fin shear layer. Therefore, in addition to the Reynolds number, three other parameters control the wake region: confinement ratio $r = (D/W)$, gap parameter $(\gamma = \Delta/D)$, and aspect ratio $(AR = L/D)$ where D is pin fin diameter, W is channel width, L is channel (pin fin) height and Δ is the distance between pin fin center and adjacent wall. Jung et al. (2012) used *μPIV* to identify flow patterns behind a bounded circular pin fin with $AR = 1.5$ centered in a rectangular microchannel with $r = 0.1$ and reported a great delay in transition from quasi-steady to unsteady wake flow up to $Re_D = 400$ $(Re_D = \rho \bar{V} D/\mu)$, where ρ is the density of water, $\bar{V}$ is the average upstream velocity in the channel and μ is dynamic viscosity of water. They supported their interpretation by comparing several flow properties like time-averaged and instantaneous velocity field, vorticity, location of stagnation points, and turbulent kinetic energy *(TKE)*. Also, shrinkage of the recirculation zone and onset of vortex shedding for $Re_D > 400$ were witnessed.

Cavitating flow downstream a pillar confined in a microchannel can create a multifaceted phenomenon that requires careful examination. To the best of the authors' knowledge, cavitation downstream a circular pillar in micro domains has not been studied before. The present study seeks to address this shortcoming through experiments. Spectral analysis performed on the time series of both the gray scale pixel intensities in the vicinity of cavity and pressure data in the center of pillar, then dominant frequency ranges were compared. To complement experimental effort and to verify pressure data measurements, single phase numerical model was developed and the results were compared to the measurements.

2. Experimental apparatus and method

2.1. The microdevice

The micro device (Fig. 1a) was fabricated by bonding a silicon substrate to a Pyrex® substrate. The microchannel had dimensions of 18.5 mm long, 1.5 mm wide, and 225 µm height. Fluid entered the channel, travelled 13.5 mm before passing a 150 µm diameter pillar, and then left the channel through the exit manifold. A scanning electron microscope *(SEM)* image of the pillar is shown in Fig. 1b.

The package (Fig. 1c), precision machined from Delrin®, was designed to contain the micro-device and provide fluidic connections to and from external fittings. O-rings were used to achieve fluidic seals with the micro-devices. The devices were held in the fixture by a 4 mm thick aluminum cover plate.

2.2. Micro fabrication

The micro-devices were fabricated using *MEMS* techniques in a clean room environment. A silicon substrate and a Pyrex wafer were processed separately and then anodically bonded together.

The micro processing started with a 450 µm thick double-side polished silicon wafer. Silicon dioxide was thermally grown on both sides of the wafer by furnace oxidation. The oxide served as a hard mask for silicon deep reactive-ion etching *(DRIE)*, and the microchannel and pillar patterns were transferred to the silicon substrate. After being etched half way through (~225 µm), the silicon wafer was flipped over; then the same etching procedure continued to etch through the holes for the fluid inlet and outlet. The silicon oxide was removed by buffered oxide etch (BOE). The patterned silicon wafer was then bonded to a Pyrex wafer to seal the microchannel from the top. Finally, each individual micro-device was separated from the bonded wafer using a die-saw machine.